LETTER

doi:10.1038/nature13028

The hippocampal CA2 region is essential for social memory

Frederick L. Hitti[1] & Steven A. Siegelbaum[1,2]

The hippocampus is critical for encoding declarative memory, our repository of knowledge of who, what, where and when[1]. Mnemonic information is processed in the hippocampus through several parallel routes involving distinct subregions. In the classic trisynaptic pathway, information proceeds from entorhinal cortex (EC) to dentate gyrus to CA3 and then to CA1, the main hippocampal output[2]. Genetic lesions of EC (ref. 3) and hippocampal dentate gyrus (ref. 4), CA3 (ref. 5) and CA1 (ref. 6) regions have revealed their distinct functions in learning and memory. In contrast, little is known about the role of CA2, a relatively small area interposed between CA3 and CA1 that forms the nexus of a powerful disynaptic circuit linking EC input with CA1 output[7]. Here we report a novel transgenic mouse line that enabled us to selectively examine the synaptic connections and behavioural role of the CA2 region in adult mice. Genetically targeted inactivation of CA2 pyramidal neurons caused a pronounced loss of social memory—the ability of an animal to remember a conspecific—with no change in sociability or several other hippocampus-dependent behaviours, including spatial and contextual memory. These behavioural and anatomical results thus reveal CA2 as a critical hub of sociocognitive memory processing.

Although the CA2 region was first described in 1934 (ref. 8), relatively little is known about its functional properties and behavioural role. To examine the importance of this region, we generated a transgenic mouse line (*Amigo2-Cre*) that expresses Cre recombinase predominantly in CA2 pyramidal neurons (PNs) in adult mice (Extended Data Fig. 1). Because this line expresses Cre throughout the brain during early development, as well as in certain limited areas outside CA2 in the adult, we stereotactically injected Cre-dependent adeno-associated virus (AAV) into the hippocampus of adult *Amigo2-Cre* mice to limit viral expression to CA2 pyramidal cells.

To determine the specificity of CA2 expression in the transgenic line, we bilaterally injected into dorsal hippocampus a Cre-dependent AAV to express yellow fluorescent protein (YFP) in Cre^+ cells (Fig. 1a). We observed selective and robust YFP expression in CA2 PNs throughout dorsal hippocampus[9–11] (Fig. 1b and Extended Data Fig. 2a). We confirmed that the Cre^+ cells were indeed CA2 PNs by demonstrating co-staining for RGS14 (ref. 12) (97.38 ± 0.31% overlap; $n = 4$ mice, 2,546 cells; Fig. 1c–e and Extended Data Fig. 3) and other known CA2 PN markers (Extended Data Fig. 2). In contrast, there was no co-staining for a CA1 PN marker (Extended Data Fig. 2). In addition, the electrophysiological properties of the YFP^+ neurons differed significantly from those of CA1 PNs (Extended Data Table 1) and largely matched the values previously reported for CA2 pyramidal neurons[7]. Only a minute fraction of YFP^+ neurons were also $GABA^+$ (0.16 ± 0.16%; $n = 3$ mice, 1,539 cells), showing the specific targeting of CA2 excitatory PNs (Fig. 1f, g and Extended Data Fig. 3). Finally, our AAV injections resulted in the targeting of the vast majority of CA2 PNs in the dorsal hippocampus, measured by the percentage of $RGS14^+$ cells that were also YFP^+ (82.33 ± 2.37%, $n = 4$ mice, 2,992 cells).

Next we mapped CA2 synaptic input and output by using viral tracing strategies that take advantage of the genetic targeting of CA2 PNs in the *Amigo2-Cre* mice, and largely confirmed results of previous studies using conventional[13] and genetic-based[14] approaches. Monosynaptic inputs to CA2 PNs were determined by trans-synpatic retrograde labelling using an EnvA pseudotyped ΔG rabies virus[15] (Extended Data Fig. 4). Unilateral viral injections revealed bilateral inputs from CA3 and CA2 (Fig. 2a, b) and strong unilateral input from both lateral and medial EC layer II neurons (Fig. 2c, d). In addition, synaptic inputs were detected from medial septum and diagonal band (Fig. 2e), median raphe nucleus (Fig. 2f), and the supramammillary nucleus of the hypothalamus (Fig. 2g).

We observed only sparse labelling of EC layer III neurons with the rabies virus approach. Our laboratory had previously concluded that EC LIII axons provide strong excitatory drive to CA2 PNs, on the basis of the finding that large excitatory postsynaptic potentials are evoked in CA2 PNs with a focal stimulating electrode placed in the stratum lacunosum of the CA1 region[7], where axons from LIII EC neurons are thought to provide the predominant source of excitatory inputs. Our present results, combined with recent results[13,14], suggest that these synaptic responses recorded in CA2 PNs may result from activation of LII fibres that course through or near the stratum lacunosum in CA1.

Output projections from CA2 were determined by expressing YFP in CA2 PNs (as in Fig. 1) and examining brains for YFP-fluorescent axons. Unilateral viral injections resulted in strong bilateral labelling in hippocampal CA1, CA2 and CA3 regions, with densest projections observed in stratum oriens and weaker projections detected in stratum radiatum (Fig. 2h, i). We did not observe extra-hippocampal outputs.

These anatomical results generally support previous[13,14] findings. However, we failed to observe vasopressinergic input to CA2 from the paraventricular nucleus of the hypothalamus[13], which may reflect an inability of the trans-synaptic rabies tracing system to label peptidergic inputs[15]. In addition, we did not observe CA2 output to the supramammillary nucleus as reported previously using conventional tracing methods[13]. We surmise that this output may represent an inhibitory projection from CA2 because our technique selectively labelled PNs. Finally, we did not observe CA2 output to EC layer II (ref. 16), perhaps because the anterograde tracing failed to detect weak connections.

To examine directly the functional and behavioural relevance of CA2, we used the *Amigo2-Cre* mouse line to inactivate output from CA2 PNs selectively. We injected into the dorsal hippocampus of the *Amigo2-Cre* mice a Cre-dependent AAV to express tetanus neurotoxin (TeNT) light chain fused to enhanced green fluorescent protein (eGFP–TeNT) in CA2 PNs to block their synaptic output. We first verified the efficacy of this approach and characterized the influence of CA2 on its CA1 PN targets by using Cre-dependent AAVs to co-express the light-activated cation channel channelrhodopsin-2 (ChR2)[17] with either TeNT or YFP. Low-intensity illumination (using 2-ms pulses of 470-nm light at 3 mW mm^{-2}) focused on CA2 reliably triggered action potentials in CA2 PNs, as seen by the presence of fast action currents in cell-attached patch clamp recordings (Fig. 3a–c). Similar rates of spiking were seen in neurons that co-expressed either YFP (Fig. 3b) or TeNT (Fig. 3c) with ChR2, indicating that the TeNT did not inhibit excitability.

[1]Department of Neuroscience, Kavli Institute, College of Physicians and Surgeons, Columbia University 1051 Riverside Drive, New York, New York 10032, USA. [2]Department of Pharmacology, Howard Hughes Medical Institute, College of Physicians and Surgeons, Columbia University 1051 Riverside Drive, New York, New York 10032, USA.

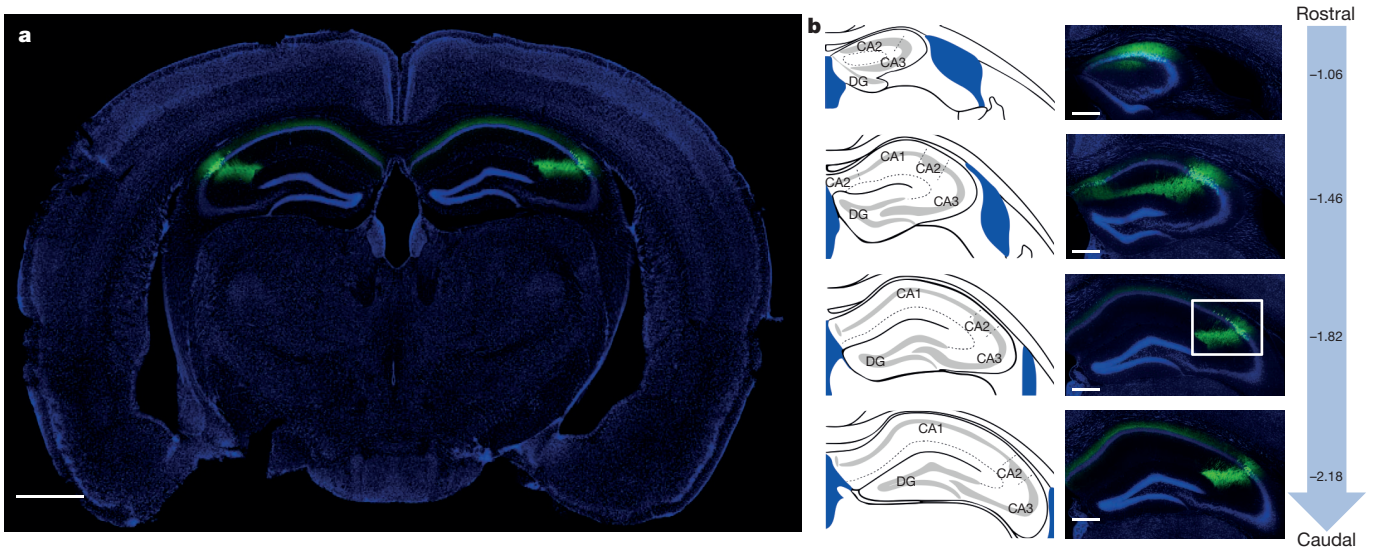

Figure 1 | Genetic targeting of the CA2 subfield using the *Amigo2-Cre* mouse line. a, Bilateral hippocampal injection of Cre-dependent YFP AAV in *Amigo2-Cre* mice resulted in specific expression of YFP (green) in CA2 PNs ($n = 64$ mice). **b**, Extent of transduction. Left: adapted reference atlas images[9]. Centre: YFP expression. Right: distance (in mm) from bregma along the rostrocaudal axis. DG, dentate gyrus. **c**–**g**, Magnified images of the boxed area in **b**. **c**, YFP (green). **d**, RGS14 staining (red, $n = 4$ mice). **e**, Merge of **c** and **d**, showing YFP and RGS14 overlap. **f**, GABA staining (red, $n = 3$ mice). **g**, Merge of **c** and **f**, showing no GABA and YFP overlap. Panels show coronal sections with Nissl counterstain (blue). Scale bars, 1,000 μm (**a**), 400 μm (**b**), 200 μm (**c**–**g**).

Next we determined the strength of synaptic transmission from CA2 to CA1 PNs by using whole-cell current-clamp recordings to measure light-evoked postsynaptic potentials (PSPs) in CA1 PNs from hippocampal slices in which ChR2 and YFP were expressed in CA2 PNs (Fig. 3d). In agreement with anatomical mapping (Fig. 2h, i) and paired recordings[7], focal photostimulation delivered to CA1 stratum oriens and stratum radiatum regions evoked robust monosynaptic PSPs (mean latency 1.22 ± 0.06 ms, $n = 119$ observations) in nearby CA1 PNs (Fig. 3e). Increasing the light intensity recruited progressively larger PSPs, presumably as a result of an increase in the number of optically activated CA2 axons (Fig. 3e, f). In stark contrast, in slices in which TeNT was co-expressed with ChR2 in CA2 PNs, illumination over a wide range of intensities produced little or no synaptic response in CA1 neurons (Fig. 3e, f), showing the efficacy of the TeNT lesion.

What are the behavioural consequences of inactivation of CA2? To address this question we compared the behaviour of control mice (CA2-YFP) with mice in which CA2 PNs were inactivated (CA2-TeNT), using viral injections in dorsal hippocampus[11]. Functional inactivation of dorsal CA2 did not alter locomotor activity or anxiety-like behaviour (Extended Data Fig. 5). Inactivation of CA2 also did not significantly alter hippocampus-dependent spatial memory assessed by the Morris water maze (although there was a trend for the CA2-inactivated mice to learn the task more slowly; Extended Data Fig. 6). Nor was there any

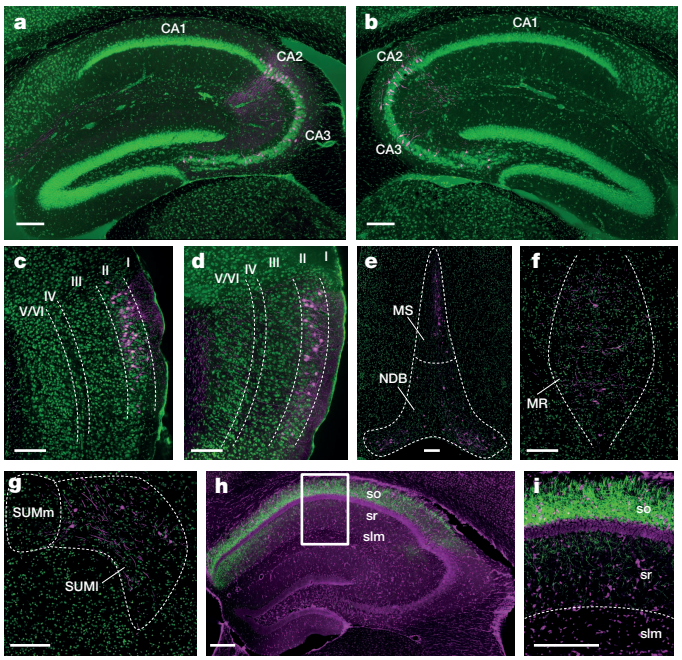

Figure 2 | Genetically targeted tracing of the CA2 circuit. a–**g**, Monosynaptic inputs to CA2 revealed with pseudotyped rabies virus ($n = 8$ mice). Cells labelled with rabies appear magenta; Nissl stain shown in green. **a**–**d**, Sagittal sections; **e**–**g**, coronal sections. **a, b**, Labelled neurons in CA2 and CA3 ipsilateral (**a**) and contralateral (**b**) to the hemisphere of rabies virus injection. Rabies labelling shows monosynaptic inputs from lateral EC (**c**), medial EC (**d**), medial septum (MS) and nucleus of the diagonal band (NDB) (**e**), median raphe (MR) (**f**) and lateral supramammillary nucleus (SUMl) (**g**). Fluorescent processes in (**c**, **d**) may represent dendritic or axonal labelling. SUMm, medial supramammillary nucleus. **h**, Output of CA2 revealed by axonal YFP signal (green, $n = 6$ mice). Nissl stain (magenta). so, stratum oriens; sr, stratum radiatum; slm, stratum lacunosum-moleculare. **i**, Magnification of boxed area in **h**. Note that CA2 makes strong projections to stratum oriens and weaker projections to stratum radiatum of CA1. Scale bars, 200 μm.

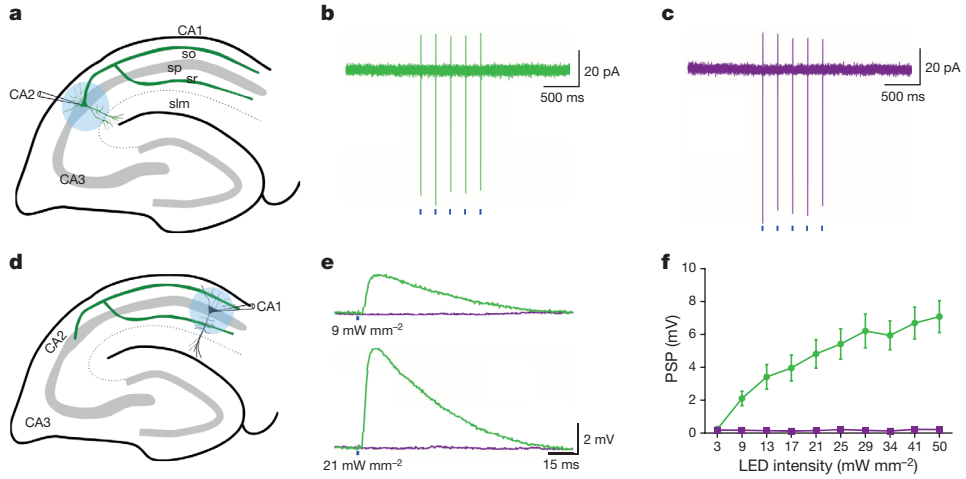

Figure 3 | Electrophysiological verification of CA2 inactivation with TeNT. **a**, Experimental setup for photostimulation of CA2 PNs. sp, stratum pyramidale. **b**, **c**, Action currents recorded from CA2 PNs expressing YFP and ChR2 ($n = 6$ neurons) (**b**) or TeNT and ChR2 ($n = 4$ neurons) (**c**) in response to five 2-ms blue (470-nm) light pulses (blue bars). **d**, Experimental setup for whole-cell current-clamp recordings of photostimulated PSPs in CA1 PNs. **e**, PSPs recorded when YFP ($n = 14$ neurons, green) or TeNT ($n = 14$ neurons, magenta) was co-expressed with ChR2 in CA2 PNs. **f**, Mean input–output curve of PSP as a function of light intensity when YFP (green) or TeNT (magenta) was co-expressed with ChR2 in CA2 PNs. Results are means ± s.e.m.

change in hippocampus-dependent contextual fear memory or amygdala-dependent auditory fear memory (Extended Data Fig. 7).

The finding that CA2 PNs integrate synaptic input from lateral EC (which conveys non-spatial information[18]) with subcortical input from both the serotonergic median raphe nucleus[19] and the hypothalamic supramammillary nucleus[20] suggests a potential role for CA2 in non-spatial hippocampal tasks. Previous studies have shown that the messenger RNA for the vasopressin 1b receptor (*Avpr1b*) is strongly expressed in CA2 (ref. 21) and that unconditional deletion of this gene impairs social recognition memory[22,23]. However, *Avpr1b* mRNA is also expressed outside hippocampus[21], and its deletion results in changes in non-hippocampus-dependent behaviours, including reduced aggression and decreased sociability[22,23], raising questions as to the selective role of CA2 in the knockout phenotype[24].

To assess directly the role of CA2 in social behaviour, we first compared the performance of CA2-YFP with that of CA2-TeNT mice in a three-chamber test of sociability[23], which examines the normal preference of a subject mouse for a chamber containing a littermate versus an empty chamber (Fig. 4a). In contrast to the effect of *Avpr1b* deletion, selective silencing of CA2 did not alter sociability as the CA2-TeNT and CA2-YFP groups displayed a significant and similar preference for the compartment containing the littermate (Fig. 4a).

In contrast to their normal sociability, CA2-TeNT mice displayed a profound deficit in social recognition as determined by a three-chamber social novelty test[23] (Fig. 4b). In this test, social recognition was measured by the increased time that a subject mouse spent interacting with a novel unrelated mouse compared with the time it spent interacting with a familiar co-housed littermate. Multiple comparison testing revealed that the CA2-YFP control group demonstrated a significant preference for the compartment containing the novel animal, whereas the CA2-TeNT group did not (Fig. 4b). Moreover, the difference score (time spent exploring the novel mouse minus the time spent exploring the familiar mouse) of the CA2-TeNT group was significantly less than that of the CA2-YFP group (Fig. 4b). This deficit was not due to a lack of interest in novelty as such, because the CA2-TeNT mice showed a normal preference for a novel object as assayed by two different novel-object-recognition protocols (Extended Data Fig. 8).

Because the social novelty test does not incorporate a defined learning phase or delay period, we next conducted a more specific test of social memory, the direct interaction test[25]. For this test a subject mouse was exposed to an unfamiliar mouse in trial 1. After a 1-h inter-trial interval, the subject mouse was either re-exposed to the same mouse as that encountered in trial 1 (Fig. 4c) or exposed to a second, unfamiliar, mouse (Fig. 4d). Social memory, measured as the decreased time that a subject mouse spends exploring a previously encountered mouse, was fully suppressed by CA2 inactivation (Fig. 4c). In contrast, CA2 silencing did not alter sociability, because CA2-YFP and CA2-TeNT subject mice showed similar and unchanging exploration times during trials 1 and 2 when two different unfamiliar mice were encountered in the two trials (Fig. 4d).

We next conducted a more stringent five-trial social memory assay[26] to confirm that CA2-inactivation abolishes social memory. In this assay, a stimulus mouse was presented to a subject mouse for four successive trials. On the fifth trial, a novel stimulus mouse was introduced (Fig. 4e). The CA2-YFP control group displayed normal social memory, as demonstrated by a marked habituation (decreased exploration) during the first four trials and a striking dishabituation (increased exploration) on presentation of a novel animal on the fifth trial. In contrast, the CA2-TeNT group showed no significant habituation during the four exposures to the stimulus mouse or dishabituation to the novel stimulus mouse, thus confirming the necessity of CA2 for social memory.

Because olfaction is crucial for normal social interaction[27], we examined whether CA2 silencing influenced the detection or recognition of non-social or social odours. CA2-TeNT mice showed no loss in the ability to detect the presence of food buried under a deep layer of cage bedding, a test of non-social odour detection (Extended Data Fig. 9a). Next we used an olfactory habituation/dishabituation test (Extended Data Fig. 9b) and found that CA2 inactivation also had no effect on the ability of mice to detect or discriminate either non-social or social odours. We therefore conclude that the deficit in social memory in the CA2-TeNT mice was not due to a defect in sensing social or non-social odours.

In this study we developed and validated an *Amigo2-Cre* mouse line that enables the precise genetic targeting of excitatory CA2 PNs, allowing us to map selectively the inputs and outputs of this largely unexplored region and demonstrate that the CA2 subfield is essential for social memory. Although we observed a fairly specific deficit in social memory after inactivation of dorsal CA2 pyramidal neurons, our results do not rule out the possibility that CA2 may participate more generally in hippocampus-dependent memory tasks. Thus, other regions of hippocampus may be able to compensate for the loss of any role that CA2 may normally have in performance of the water maze or contextual fear-conditioning tasks. Alternatively, CA2 may be selectively required for the performance of more demanding non-social memory tasks.

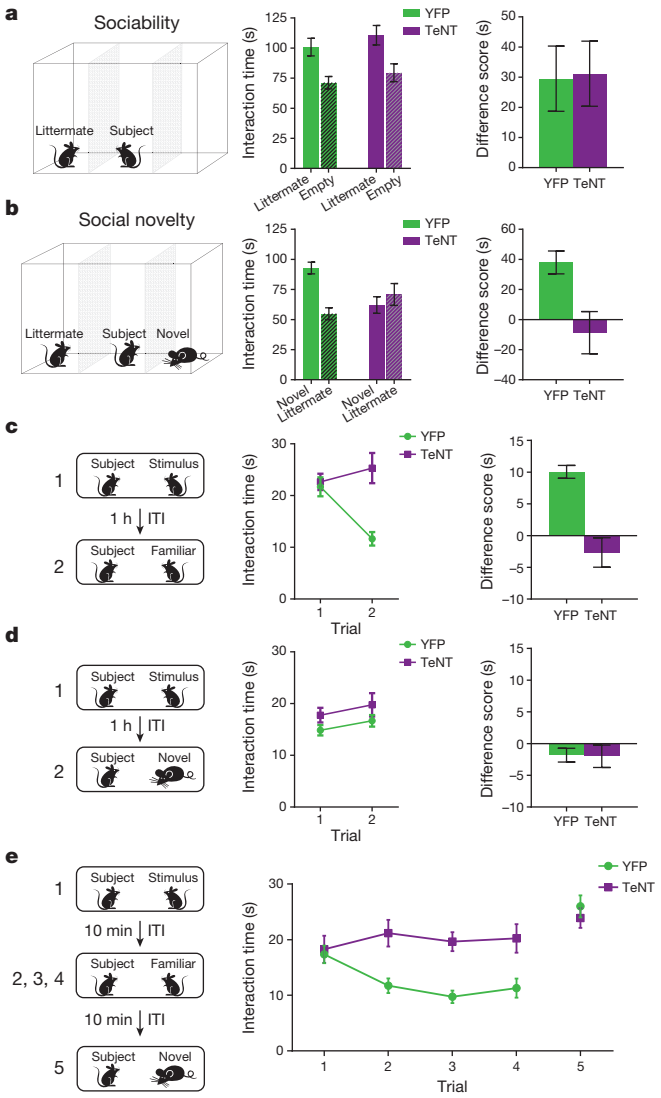

Figure 4 | Inactivation of CA2 impairs social memory. **a**, Left: sociability test. Middle: YFP ($n = 11$) and TeNT ($n = 13$) mice preferred the littermate chamber (YFP, $P = 0.0083$; TeNT, $P = 0.0055$; multiplicity-adjusted P values), with no significant difference in interaction times (two-way analysis of variance (ANOVA): treatment × chamber $F(1,44) = 0.013$, $P = 0.91$; treatment $F(1,44) = 1.566$, $P = 0.22$; chamber $F(1,44) = 17.49$, $P = 0.0001$). Right: interaction time difference scores (littermate minus empty) were similar ($P = 0.9154$, two-tailed Student's t-test). **b**, Left: social novelty test. Middle: only YFP mice preferred the novel animal over a littermate (YFP, $P = 0.0012$; TeNT, $P = 0.3593$; multiplicity-adjusted P values); the groups differed significantly (ANOVA: treatment × chamber $F(1,44) = 11.25$, $P = 0.0016$). Right: difference score (novel minus littermate) of TeNT group was significantly less than that of YFP group ($P = 0.0109$, two-tailed Student's t-test). **c**, **d**, Left: direct interaction test using identical (**c**) or different (**d**) stimulus animals in the two trials. **c**, Middle: only YFP mice displayed decreased investigation during trial 2 of mouse encountered in trial 1 (YFP, $n = 15$, $P < 0.0001$; TeNT, $n = 16$, $P = 0.1499$; multiplicity-adjusted P values); the groups differed significantly (ANOVA: treatment × trial $F(1,29) = 24.23$, $P < 0.0001$). Right: TeNT group difference score (trial 1 minus trial 2) was less than that of YFP group ($P < 0.0001$; two-tailed Student's t-test). **d**, Middle: the two groups explored two different stimulus animals similarly (ANOVA: treatment × trial $F(1,29) = 0.0068$, $P = 0.93$; treatment $F(1,29) = 2.405$, $P = 0.13$; trial $F(1,29) = 3.278$, $P = 0.0806$), with similar difference scores (right, $P = 0.93$, two-tailed Student's t-test). **e**, Five-trial social memory assay. YFP ($n = 15$), but not TeNT ($n = 14$), mice habituated to same mouse (trials 1–4) and dishabituated to a novel mouse (trial 5). The groups differed significantly (ANOVA: treatment × trial $F(4,108) = 7.26$, $P < 0.0001$; treatment $F(1,27) = 7.86$, $P = 0.009$; trial $F(4,108) = 15.41$, $P < 0.0001$). ITI, inter-trial interval. Results are means ± s.e.m.

The importance of human hippocampus for social memory is famously illustrated by the case of Henry Molaison (patient H.M.), who, after bilateral medial temporal lobe ablation, could not form new memories of people he had worked with for years[28]. Lesions limited to the hippocampus also impair social memory in both humans[1] and rodents[25]. Because several neuropsychiatric disorders are associated with altered social endophenotypes, our findings raise the possibility that CA2 dysfunction may contribute to these behavioural changes. This possibility is supported by findings of a decreased number of CA2 inhibitory neurons in individuals with schizophrenia and bipolar disorder[29], and altered vasopressin signalling in autism[30]. Thus, CA2 may provide a new target for therapeutic approaches to the treatment of social disorders.

METHODS SUMMARY

Generation of *Amigo2-Cre* mouse line. A bacterial artificial chromosome (BAC) was modified to insert a Cre-HSV-polyA cassette at the translational start of *Amigo2*. Six B6CBA/F2 founders were generated. One line that selectively expressed Cre in CA2 of adult mice was backcrossed to C57BL/6J a minimum of six times and used in these experiments.

Subjects. Cre^+ males were bred to C57BL/6J females to keep the *Amigo2-Cre* line hemizygous on the C57BL/6J background. Only Cre^+ males were used for experiments, which were conducted 2–4 weeks after viral injection and approved by the Columbia University Institutional Animal Care and Use Committee.

Viruses. AAV5-EF1α-FLEx-eYFP-WPRE-hGH, AAV5-EF1α-FLEx-TVA-mCherry-WPRE-hGH and AAV5-CAG-FLEx-rabiesG-WPRE-hGH were obtained from the University of North Carolina vector core. (EnvA)SAD-ΔG-mCherry was produced at Columbia. AAV5-EF1α-FLEx-hChR2(H134R)-EYFP-WPRE and AAV5-EF1α-FLEx-eGFP-TeNT-WPRE-hGH were obtained from the UPenn vector core.

Stereotaxic injection. Male mice (more than 8 weeks old) were anaesthetized with isoflurane, and virus was injected into the dorsal hippocampus at −1.6 mm anteroposterior, ±1.6 mm mediolateral, and −1.7 mm dorsoventral relative to bregma.

Electrophysiology. Two to three weeks after AAV injection, hippocampal slices 400 μm thick were prepared. Blue light was delivered through a 20× objective to activate ChR2. Patch membrane voltage was held at −70 mV for cell-attached voltage-clamp recordings. Whole-cell recordings were obtained from CA1 PNs in current-clamp mode with membrane at initial resting potential.

Behavioural tests. Two to five male *Amigo2-Cre* mice were housed per cage with *ad libitum* access to food and water. Tests were conducted during the light cycle. Half of the mice in each cage were injected with the YFP virus, and the other half were injected with the TeNT virus. The experimenter was blind to the group identities. Open field activity was recorded with Activity Monitor. The direct interaction, five-trial social memory and olfactory tests were scored online by the experimenter. All other tests were scored automatically by ANY-maze.

Online Content Any additional Methods, Extended Data display items and Source Data are available in the online version of the paper; references unique to these sections appear only in the online paper.

Received 5 December 2013; accepted 10 January 2014.
Published online 23 February 2014.

1. Squire, L. R. & Wixted, J. T. The cognitive neuroscience of human memory since H.M. *Annu. Rev. Neurosci.* **34,** 259–288 (2011).
2. van Strien, N. M., Cappaert, N. L. & Witter, M. P. The anatomy of memory: an interactive overview of the parahippocampal–hippocampal network. *Nature Rev. Neurosci.* **10,** 272–282 (2009).
3. Suh, J., Rivest, A. J., Nakashiba, T., Tominaga, T. & Tonegawa, S. Entorhinal cortex layer III input to the hippocampus is crucial for temporal association memory. *Science* **334,** 1415–1420 (2011).
4. Nakashiba, T. *et al.* Young dentate granule cells mediate pattern separation, whereas old granule cells facilitate pattern completion. *Cell* **149,** 188–201 (2012).
5. Nakashiba, T., Young, J. Z., McHugh, T. J., Buhl, D. L. & Tonegawa, S. Transgenic inhibition of synaptic transmission reveals role of CA3 output in hippocampal learning. *Science* **319,** 1260–1264 (2008).
6. Tsien, J. Z., Huerta, P. T. & Tonegawa, S. The essential role of hippocampal CA1 NMDA receptor-dependent synaptic plasticity in spatial memory. *Cell* **87,** 1327–1338 (1996).
7. Chevaleyre, V. & Siegelbaum, S. A. Strong CA2 pyramidal neuron synapses define a powerful disynaptic cortico-hippocampal loop. *Neuron* **66,** 560–572 (2010).
8. Lorente de Nó, R. Studies on the structure of the cerebral cortex. II. Continuation of the study of the ammonic system. *J. Psychol. Neurol.* **46,** 113–177 (1934).
9. Franklin, K. & Paxinos, G. *The Mouse Brain in Stereotaxic Coordinates* (Academic, 2007).

10. Lein, E. S., Callaway, E. M., Albright, T. D. & Gage, F. H. Redefining the boundaries of the hippocampal CA2 subfield in the mouse using gene expression and 3-dimensional reconstruction. *J. Comp. Neurol.* **485,** 1–10 (2005).
11. Fanselow, M. S. & Dong, H. W. Are the dorsal and ventral hippocampus functionally distinct structures? *Neuron* **65,** 7–19 (2010).
12. Lee, S. E. *et al.* RGS14 is a natural suppressor of both synaptic plasticity in CA2 neurons and hippocampal-based learning and memory. *Proc. Natl Acad. Sci. USA* **107,** 16994–16998 (2010).
13. Cui, Z., Gerfen, C. R. & Young, W. S. III. Hypothalamic and other connections with dorsal CA2 area of the mouse hippocampus. *J. Comp. Neurol.* **521,** 1844–1866 (2013).
14. Kohara, K. *et al.* Cell type-specific genetic and optogenetic tools reveal hippocampal CA2 circuits. *Nature Neurosci.* 10.1038/nn.3614 (2013).
15. Wall, N. R., De La Parra, M., Callaway, E. M. & Kreitzer, A. C. Differential innervation of direct- and indirect-pathway striatal projection neurons. *Neuron* **79,** 347–360 (2013).
16. Rowland, D. C. *et al.* Transgenically targeted rabies virus demonstrates a major monosynaptic projection from hippocampal area CA2 to medial entorhinal layer II neurons. *J. Neurosci.* **33,** 14889–14898 (2013).
17. Boyden, E. S., Zhang, F., Bamberg, E., Nagel, G. & Deisseroth, K. Millisecond-timescale, genetically targeted optical control of neural activity. *Nature Neurosci.* **8,** 1263–1268 (2005).
18. Hargreaves, E. L., Rao, G., Lee, I. & Knierim, J. J. Major dissociation between medial and lateral entorhinal input to dorsal hippocampus. *Science* **308,** 1792–1794 (2005).
19. Hensler, J. G. Serotonergic modulation of the limbic system. *Neurosci. Biobehav. Rev.* **30,** 203–214 (2006).
20. Pan, W. X & McNaughton, N. The supramammillary area: its organization, functions and relationship to the hippocampus. *Prog. Neurobiol.* **74,** 127–166 (2004).
21. Young, W. S., Li, J., Wersinger, S. R. & Palkovits, M. The vasopressin 1b receptor is prominent in the hippocampal area CA2 where it is unaffected by restraint stress or adrenalectomy. *Neuroscience* **143,** 1031–1039 (2006).
22. Wersinger, S. R., Ginns, E. I., O'Carroll, A. M., Lolait, S. J. & Young, W. S. III. Vasopressin V1b receptor knockout reduces aggressive behavior in male mice. *Mol. Psychiatry* **7,** 975–984 (2002).
23. DeVito, L. M. *et al.* Vasopressin 1b receptor knock-out impairs memory for temporal order. *J. Neurosci.* **29,** 2676–2683 (2009).
24. Stevenson, E. L. & Caldwell, H. K. The vasopressin 1b receptor and the neural regulation of social behavior. *Horm. Behav.* **61,** 277–282 (2012).
25. Kogan, J. H., Frankland, P. W. & Silva, A. J. Long-term memory underlying hippocampus-dependent social recognition in mice. *Hippocampus* **10,** 47–56 (2000).
26. Ferguson, J. N. *et al.* Social amnesia in mice lacking the oxytocin gene. *Nature Genet.* **25,** 284–288 (2000).
27. Brennan, P. A. & Zufall, F. Pheromonal communication in vertebrates. *Nature* **444,** 308–315 (2006).
28. Corkin, S. What's new with the amnesic patient H.M.? *Nature Rev. Neurosci.* **2,** 153–160 (2002).
29. Benes, F. M., Kwok, E. W., Vincent, S. L. & Todtenkopf, M. S. A reduction of nonpyramidal cells in sector CA2 of schizophrenics and manic depressives. *Biol. Psychiatry* **44,** 88–97 (1998).
30. Meyer-Lindenberg, A., Domes, G., Kirsch, P. & Heinrichs, M. Oxytocin and vasopressin in the human brain: social neuropeptides for translational medicine. *Nature Rev. Neurosci.* **12,** 524–538 (2011).

Acknowledgements We thank T. R. Reardon for providing the rabies virus; J. Kupferman and F. Lema for experimental assistance; and C. Denny, Z. Donaldson, R. Hen, J. Gordon, J. Basu and M. Russo for discussions and comments on the manuscript. This work was supported by a Ruth L. Kirschstein F30 National Research Service Award from the National Institute of Mental Health (F.L.H.) and the Howard Hughes Medical Institute (S.A.S.).

Author Contributions F.L.H. planned and performed the experiments, analysed the data and wrote the manuscript. S.A.S. oversaw the overall execution of the project, contributed to the experimental design and the interpretation of the data, provided financial support and helped write the manuscript.

Author Information Reprints and permissions information is available at www.nature.com/reprints. The authors declare no competing financial interests. Readers are welcome to comment on the online version of the paper. Correspondence and requests for materials should be addressed to S.A.S. (sas8@columbia.edu).

METHODS

Generation of *Amigo2-Cre* mouse line. Selective expression of *Amigo2* in the CA2 region of hippocampus was identified on the basis of GENSAT[31] and Allen Brain Atlas[32] data. The RP23-288P18 bacterial artificial chromosome (BAC) that contained the *Amigo2* gene and its surrounding regulatory elements was obtained from the BACPAC Resource Center[33]. Recombineering with galK selection and the SW102 bacterial strain[34] was employed to modify RP23-288P18 seamlessly so that a Cre-HSV-poly(A) cassette was inserted at the translation start site of the *Amigo2* gene. Specifically, the Cre expression cassette was amplified by polymerase chain reaction from pLD53.SC-Cre (ref. 35). The homology arms used for the recombineering were 5′-ATTGGTGGGAGACTGAGCTGATGAGAAGCGACT GGCAAGAGACTCAGAGGCGACCATA-3′ (5′ arm) and 5′-ATGTCGTTAAG GTTCCACACACTGCCCACCCTGCCTAGAGCTGTCAAACCGGGTTGCAG AGA-3′ (3′ arm). This modified BAC was injected into B6CBA/F2 pronuclei, and embryos were implanted into pseudopregnant females. PCR was used to identify the offspring that were Cre-positive. These founders were crossed to the Ai14 Cre-reporter line[36] to examine the specificity of Cre expression. At 12 weeks of age, the Cre^+ offspring were perfused transcardially with 4% paraformaldehyde (PFA) in PBS, and expression of tdTomato was examined in 50-μm coronal slices. CA2-specific expression of tdTomato was not observed in any of the founder lines. However, injection of the EF1α-FLEx-eYFP-WPRE-hGH Cre-reporter AAV into the hippocampus of adult mice (more than 8 weeks old) revealed CA2-specific expression in one of the six founder lines. This line was used for all of the studies presented here. The line was backcrossed to C57BL/6J a minimum of six times before any behavioural or physiological experiments were performed.

Subjects. The *Amigo2-Cre* line was maintained as a hemizygous line on the C57BL/6J background by breeding Cre^+ males to C57BL/6J females. Only Cre^+ males were used for these experiments. Mice more than 8 weeks old were injected with virus under stereotactic control into the hippocampus proper to avoid *Amigo2-Cre* expression in mossy cells of the dentate gyrus. All anatomical, behavioural and physiological experiments were conducted 2–4 weeks after injection. All procedures were approved by the Institutional Animal Care and Use Committee at Columbia University and the New York State Psychiatric Institute.

Virus constructs. AAV5-EF1α-FLEx-eYFP-WPRE-hGH (4×10^{12} virus molecules ml^{-1}) was injected to label CA2 PNs and trace their axons. (EnvA)SAD-ΔG-mCherry (10^8 infectious particles ml^{-1}) pseudotyped rabies virus was produced as described previously[37] and used to label monosynaptic inputs to CA2. This virus can only infect cells expressing the TVA receptor[37,38]. Before rabies virus injection, AAV5-EF1α-FLEx-TVA-mCherry-WPRE-hGH[38] (3×10^{12} virus molecules ml^{-1}) was injected to express TVA in CA2. To permit retrograde synaptic transport of the ΔG virus, AAV5-CAG-FLEx-rabiesG-WPRE-hGH[38] (2×10^{12} virus molecules ml^{-1}) was co-injected with the TVA virus to express G in CA2. The aforementioned AAVs were obtained from the University of North Carolina vector core. To specifically excite CA2 PNs, AAV5-EF1α-FLEx-hChR2(H134R)-EYFP-WPRE-hGH (2×10^{12} genome copies ml^{-1}) was injected to express ChR2 in the CA2 neurons. This vector was obtained from the University of Pennsylvania (UPenn) vector core. To ablate CA2 pyramidal cell output, tetanus neurotoxin light chain (TeNT) was expressed selectively in these cells. A Cre-dependent AAV vector carrying eGFP–TeNT was created by PCR amplifying eGFP–TeNT from pTRE2-eGFP-TeNT-PEST[39] and subcloning it into pAAV-EF1α-DIO-hChR2-mCherry-WPRE (Addgene plasmid 20297) between the NheI and AscI sites in the inverse orientation. The resulting vector, pAAV-EF1α-FLEx-eGFP-TeNT-WPRE-hGH, was sent to the UPenn vector core for custom production of AAV5-EF1α-FLEx-eGFP-TeNT-WPRE-hGH (10^{13} genome copies ml^{-1}).

Stereotaxic injection. Mice were anaesthetized with isoflurane (2–5%) and placed in a stereotaxic apparatus (Digital Just for Mice Stereotaxic Instrument). The head was fixed and the skull was exposed. Burr holes were made and a glass micropipette (Drummond Scientific) was slowly lowered into the dorsal hippocampus at −1.6 mm anteroposterior, ±1.6 mm mediolateral and −1.7 mm dorsoventral relative to bregma. The pipettes were formed with 20-μm diameter tips using a P-2000 laser puller (Sutter Instrument). For the mouse line validation, anterograde tracing and behavioural experiments, 180 nl of virus was pressure-injected into each hemisphere. For the retrograde tracing experiments, 180 nl of a 1:5 mix of the TVA and rabies G AAV vectors was injected unilaterally. For the electrophysiological experiments, 360 nl of a 1:1 mix of ChR2 AAV and either YFP or TeNT AAV was injected. After injection, the pipette remained in place for 5 min and was then slowly retracted. The mice were placed on a heating pad (TR-200; Fine Science Tools) throughout the duration of the surgery. After injection, the scalp was sutured, saline was administered subcutaneously, and buprenorphine (0.05–0.1 mg kg^{-1}) was administered intraperitoneally for analgesia. The mice were placed under heating lamps during recovery from anaesthesia. For the retrograde tracing experiments, these procedures were repeated 2 weeks after the initial AAV injection to inject 360 nl of (EnvA)SAD-ΔG-mCherry rabies virus. To test the specificity of the rabies virus, a subset of animals was injected with 360 nl of the (EnvA)SAD-ΔG-mCherry rabies virus without previous injection of AAVs expressing TVA and G. All injections were verified histologically. No injections were mistargeted; hence no subjects were excluded from analysis as a result of injection failure.

Immunohistochemistry and confocal microscopy. Mice were administered ketamine/xylazine (150 mg kg^{-1}, 10 mg kg^{-1}, respectively) and perfused transcardially with ice-cold PBS followed by ice-cold 4% PFA in PBS. Brains were postfixed overnight in 4% PFA in PBS and 50-μm slices were prepared (Vibratome 3000 Plus; The Vibratome Company). Antigen retrieval[40] was performed for RGS14 staining. In brief, free-floating sections were incubated at 80 °C for 30 min in 50 mM sodium citrate pH 8.5. Slices were permeabilized with 0.2% Triton X-100 in PBS and blocked with 10% goat serum in PBS. The sections were incubated overnight at 4 °C in primary antibody (1:50 dilution; 73-170; NeuroMab,). For PCP4 (ref. 10), STEP[41], WFS[42] and GABA staining, sections were permeabilized and blocked as above and then incubated overnight at 4 °C in primary antibodies against PCP4 (1:200 dilution; HPA005792; Sigma-Aldrich), STEP (1:500 dilution; 4396; Cell Signaling Technology), WFS1 (1:250 dilution; 11558-1-AP; Proteintech) or GABA (1:500 dilution; A2052; Sigma-Aldrich). Sections were washed the following day and incubated for 2 h with Alexa 555 or 647 secondary antibodies (1:500 dilution; A21422, A21428, or A21245; Invitrogen) and NeuroTrace (1:250 dilution; N21479 or N21483; Invitrogen). Slices were then mounted with either Prolong Gold (P36930; Invitrogen) or VECTASHIELD (H-1000; Vector Laboratories) and imaged. An inverted laser scanning confocal microscope (LSM 700; Zeiss) was used for fluorescence imaging, followed by analysis in ImageJ[43]. For cell counting experiments, every fifth slice throughout the rostral half of the hippocampus (five slices in total) was examined. The first section was randomly chosen, and cells were assessed for double labelling in a single optical section taken near the middle of the slice.

Electrophysiology. Two to three weeks after AAV injection, mice were anaesthetized with isoflurane (5%) and perfused transcardially with an ice-cold dissection solution that contained (in mM): 10 NaCl, 195 sucrose, 2.5 KCl, 10 glucose, 25 $NaHCO_3$, 1.25 NaH_2PO_4, 2 sodium pyruvate, 0.5 $CaCl_2$ and 7 $MgCl_2$. The hippocampi were dissected out and 400-μm thick slices were cut (VT1200S; Leica) perpendicular to the longitudinal axis of the hippocampus. The slices were then transferred to a chamber containing a 1:1 mixture of dissection solution and artificial cerebrospinal fluid (aCSF). The aCSF contained (in mM): 125 NaCl, 2.5 KCl, 22.5 glucose, 25 $NaHCO_3$, 1.25 NaH_2PO_4, 3 sodium pyruvate, 1 ascorbic acid, 2 $CaCl_2$ and 1 $MgCl_2$. Slices were incubated at 30 °C for 30 min and then at 19–21 °C for at least 1.5 h before recording. Slices were transferred to a recording chamber (Warner Instruments), perfused with aCSF and maintained at 33 °C. All solutions were saturated with carbogen (95% O_2 and 5% CO_2). Whole-cell recordings were obtained from PNs with a patch pipette (3–5 MΩ) containing (in mM): 135 $KMeSO_4$, 5 KCl, 0.1 EGTA-Na, 10 HEPES, 2 NaCl, 5 ATP, 0.4 GTP, 10 phosphocreatine at pH 7.2 and osmolarity 280–290 mosM. Series resistance, which was always less than 30 MΩ, was monitored and compensated for throughout the experiment. Cells with a 15% or greater change in series resistance were excluded from analysis. To activate ChR2, 2-ms pulses of blue (470-nm) light (M470L2-C1; Thor Labs) were delivered through a 20× objective. Light power from the objective was measured with a power meter (PM100D; Thor Labs). The objective was centred on the neuron that was being recorded during the experiment. For the CA2 cell-attached recordings, a gigaohm seal was made and action currents were measured in voltage-clamp mode (patch membrane voltage held at −70 mV) while five pulses of blue light were delivered. For the input–output curves, whole-cell recordings were made from CA1 PNs in current-clamp mode with the initial membrane voltage at the resting potential; the objective was centred on the patched CA1 neuron. This provided illumination over stratum oriens, stratum pyramidale and stratum radiatum, thus activating the CA2 projections to CA1 that course through stratum oriens and stratum radiatum.

Behavioural tests. Mice were housed two to five in each cage and were given *ad libitum* access to food and water. They were kept on a 12-h (6:00 to 18:00) light–dark cycle in a room maintained at 21 °C. All tests were conducted during the light cycle. Mice were habituated to handling and transport from the colony room to the behavioural room for 3 days before behavioural tests were begun. Mice were given 1 h to habituate after transport to the behavioural room before any tests were conducted. The experimenter was blind to the treatment groups. The control group (CA2-YFP) was injected with AAV5-EF1α-FLEx-eYFP-WPRE-hGH; the CA2-inactivated group (CA2-TeNT) was injected with AAV5-EF1α-FLEx-eGFP-TeNT-WPRE-hGH. To blind the experimenter and randomize the treatment groups, virus aliquots were stored as pairs of coded cryotubes. Half of the mice in each home cage were injected with the YFP virus, and the other half were injected with the TeNT virus. The identity of the groups was revealed only after testing was completed. For the elevated plus maze, novel object, Morris water maze and three-chamber tests, mice were tracked with an overhead FireWire camera (DMK 31AF03-Z2; The Imaging Source) and ANY-maze (Stoelting). Freezing

during fear conditioning was tracked with a Fire-i (Unibrain) camera and analysed with ANY-maze. All apparatuses and testing chambers were cleaned with 70% propan-2-ol wipes (VWR) between animals unless otherwise indicated below.

Open field. Mice were placed in an open field (ENV-510S; Med Associates, Inc.) for 30 min, and locomotor and rearing activity was monitored by means of infrared beam breaks and recorded by Activity Monitor (Med Associates, Inc.) software. The entire apparatus was enclosed in a sound-attenuating cubicle.

Elevated plus maze. Mice were placed in the centre of a maze (Stoelting) constructed in the shape of a plus with two enclosed arms (walls 15 cm high) and two open arms. The maze was elevated 40 cm from the ground. Mice were allowed to explore the maze for 8 min. Entry into an arm was scored only after 85% of the animal's tracked body area was in the arm.

Novel object. Two variations of the novel-object task were run. Both were conducted in an arena 50 cm long, 25 cm wide and 30.5 cm high. For both tests, the snouts of the mice were tracked and object interaction was measured as time spent with snout within 2 cm of the object. The objects (a glass chess piece, a small metal lock and a small plastic box) were secured to the arena with neodymium magnets to render them immovable. In the first variation, mice were habituated to the arena and objects 1 and 2 over the course of four 5-min trials separated by an inter-trial interval of 10 min. Mice were then tested for object recognition memory 1 h after the fourth trial during the 5-min-long fifth trial. Either object 1 or object 2 (counterbalanced) was swapped for object 3 during the fifth trial. In the second variation of this test, the mice were habituated to the empty arena for 10 min each day for three consecutive days. On day 4, the mice were exposed to a pair of either object 1 or object 2 for 5 min. Object recognition memory was tested 1 h after this trial by exposure to objects 1 and 2 for 5 min. In both protocols, object recognition memory was measured as the increased time spent investigating the novel object.

Morris water maze. The Morris water maze task was run over the course of 14 days in a pool 120 cm in diameter filled with water that was opacified with non-toxic white paint (Prang tempera paint; VWR). The water was maintained at 19–20 °C. Four 1-min trials were administered each day, and mice were run in groups of eight. On days 1 and 2 cued learning was conducted. During this procedure, mice were trained to find a circular platform (10 cm in diameter) submerged 1 cm below the surface of the water and marked with a flag. Distal cues in the room were obscured by a black curtain that encircled the tank. The mouse was removed from the tank and returned to its home cage 15 s after locating the platform. If a mouse failed to locate the platform during the 1-min trial, it was gently guided towards the platform. The mice were released from different start points at the beginning of each trial, and the platform location also varied between trials. On days 3–7 the flag was removed from the platform, rendering it hidden, and the curtains were removed, which allowed the mice to now use distal cues to locate the hidden platform. The platform was kept in the middle of the southwest quadrant of the maze during days 3–7. On day 8, spatial memory was assayed with a 1-min probe trial in which the platform was removed. Reversal training was conducted on days 9–13 with the platform now hidden in the northwest quadrant. Spatial memory of the novel location was tested with a 1 min probe trial on day 14. Release and platform locations were adapted from previous studies[44].

Fear conditioning. A three-day delay fear-conditioning protocol was employed to test hippocampus-dependent contextual fear memory and amygdala-dependent auditory fear memory. On day 1 the mice were placed in an enclosure (17 cm × 17 cm × 25 cm) with a steel grid floor. This enclosure was located in a sound-attenuating chamber that contained a FireWire camera, a light and a speaker. On day 1 the enclosure was outfitted as context A, which consisted of three Plexiglas walls and one opaque wall with black and white stripes. Acetic acid (1%) was placed as the dominant odour, and the house fan was turned on. The enclosure was cleaned with 70% propan-2-ol between animals. Mice were moved from their home cage to a transfer cage with no bedding and after 15–20 s were placed in the fear-conditioning chamber. After 150 s, a tone (30 s, 2.8 kHz, 85 dB) was played and co-terminated with a shock (2 s, 0.7 mA). Mice were removed from the chamber 30 s after the shock. On day 2 contextual fear memory was assayed by placing the mice back in context A for 300 s. On day 3 the mice were brought to the testing room, which was now dimly illuminated with red light. The mice were placed in context B, which consisted of an enclosure with three solid grey coloured walls, one Plexiglas wall with a circular door, and a red, flat plastic roof. The floor of the enclosure was a white piece of plastic, 0.25% benzaldehyde was the dominant odour, and the enclosure was cleaned between animals with Vimoba. Mice were first moved from their home cage to a circular bucket and then to the testing chamber. After 180 s, the tone from day 1 was sounded for 60 s. The percentage of time spent freezing (defined as the absence of all movement except for respiration) was measured throughout these experiments and served as an index of fear memory.

Sociability and social novelty. This test was performed as described previously[23]. In brief, mice were placed in an arena divided into three equal-sized compartments by plastic mesh. On day 1 a 5-min sociability trial was conducted. A littermate was placed in the left or right compartment (systematically alternated) and the test subject was placed into the centre compartment. The time that the test subject spent investigating each compartment (snout within 2 cm of the mesh barrier) was measured, and a difference score was computed. On day 2 a 5-min social novelty test was conducted in which a littermate was placed in either the left or right compartment, and a novel animal (C57BL/6J, 3 months old, male) was placed in the other compartment. The test subject was placed in the centre compartment, investigation time was measured, and a difference score, determined by subtracting the time spent investigating the two compartments, was computed.

Direct interaction. This test was adapted from ref. 25. Under low light (12 lux), mice were placed in a standard clean cage, and a novel mouse (C57BL/6J, 4-5-week-old, male) was introduced. Activity was monitored for 5 min and scored online for social behaviour (anogenital and nose-to-nose sniffing, following and allogrooming) initiated by the test subject. After an inter-trial interval of 1 h, the test was run again with either the previously encountered mouse or a novel mouse. The time spent in social interaction during trial 1 was subtracted from the social interaction time during trial 2 to obtain the difference score.

Five-trial social memory assay. This test was run as described previously[26,45]. In brief, subject mice were individually housed for 7 days before testing. On the day of testing, the subjects were presented with a 10-week-old CD-1 ovariectomized female mouse for four successive 1-min trials. On the fifth trial, a novel stimulus animal was presented.

Buried food test. To ensure palatability of the food, mice were given 1 g reward treats (F05472-1; Bio-Serv) in their home cages 1 day before testing. All pellets were consumed. The mice were then food-deprived for 18 h before the test, to improve sensitivity[46]. A treat was hidden under 1.5 cm of standard cage bedding, a mouse was placed in the cage, and the latency to consumption of the treat was recorded.

Olfactory habituation/dishabituation test. This test was run as described previously[46], with the exclusion of the first three trials in which a water-soaked cotton swab is presented. A trained observer measured and recorded olfactory investigation of the odorant-soaked cotton swabs.

Statistical analysis. Prism 6 (GraphPad) was used for statistical analysis and to graph data. Statistical significance was assessed by two-tailed unpaired Student's *t*-tests, two-way ANOVA, or two-way repeated-measures ANOVA where appropriate. Significant main effects or interactions were followed up with multiple comparison testing with the use of Holm–Sidak's correction. Results were considered significant when $P < 0.05$. α was set equal to 0.05 for multiple comparison tests. Sample sizes were chosen on the basis of previous studies. Data met assumptions of statistical tests, and variance was similar between groups for all metrics measured except for action potential duration (Extended Data Table 1), social novelty difference score (Fig. 4b) and direct interaction difference score (Fig. 4c).

31. Heintz, N. *GENSAT Brain Atlas of gene expression in EGFP Transgenic Mice* http://www.gensat.org (2003).
32. Lein, E. S. *ISH Data: Allen Brain Atlas: Mouse Brain* http://mouse.brain-map.org/ (2007).
33. de Jong, P. J. *BAC Clones Distribution Center – BACPAC Resources Center* https://bacpac.chori.org/ (2000).
34. Warming, S., Costantino, N., Court, D. L., Jenkins, N. A. & Copeland, N. G. Simple and highly efficient BAC recombineering using galK selection. *Nucleic Acids Res.* **33,** e36 (2005).
35. Gong, S. *et al.* Targeting Cre recombinase to specific neuron populations with bacterial artificial chromosome constructs. *J. Neurosci.* **27,** 9817–9823 (2007).
36. Madisen, L. *et al.* A robust and high-throughput Cre reporting and characterization system for the whole mouse brain. *Nature Neurosci.* **13,** 133–140 (2010).
37. Wickersham, I. R., Sullivan, H. A. & Seung, H. S. Production of glycoprotein-deleted rabies viruses for monosynaptic tracing and high-level gene expression in neurons. *Nature Protocols* **5,** 595–606 (2010).
38. Watabe-Uchida, M., Zhu, L., Ogawa, S. K., Vamanrao, A. & Uchida, N. Whole-brain mapping of direct inputs to midbrain dopamine neurons. *Neuron* **74,** 858–873 (2012).
39. Yamamoto, M. *et al.* Reversible suppression of glutamatergic neurotransmission of cerebellar granule cells *in vivo* by genetically manipulated expression of tetanus neurotoxin light chain. *J. Neurosci.* **23,** 6759–6767 (2003).
40. Jiao, Y. *et al.* A simple and sensitive antigen retrieval method for free-floating and slide-mounted tissue sections. *J. Neurosci. Methods* **93,** 149–162 (1999).
41. Boulanger, L. M. *et al.* Cellular and molecular characterization of a brain-enriched protein tyrosine phosphatase. *J. Neurosci.* **15,** 1532–1544 (1995).
42. Takeda, K. *et al.* WFS1 (Wolfram syndrome 1) gene product: predominant subcellular localization to endoplasmic reticulum in cultured cells and neuronal expression in rat brain. *Hum. Mol. Genet.* **10,** 477–484 (2001).
43. Rasband, W. S. *Image J.* http://imagej.nih.gov/ij/ (1997).
44. Vorhees, C. V. & Williams, M. T. Morris water maze: procedures for assessing spatial and related forms of learning and memory. *Nature Protocols* **1,** 848–858 (2006).
45. Bielsky, I. F., Hu, S., Szegda, K. L., Westphal, H. & Young, L. J. Profound impairment in social recognition and reduction in anxiety-like behavior in vasopressin V1a receptor knockout mice. *Neuropsychopharmacology* **29,** 483–493 (2004).
46. Yang, M. & Crawley, J. N. Simple behavioral assessment of mouse olfaction. *Curr. Protocols Neurosci.* **84,** 8.24.1–8.24.12 (2009).

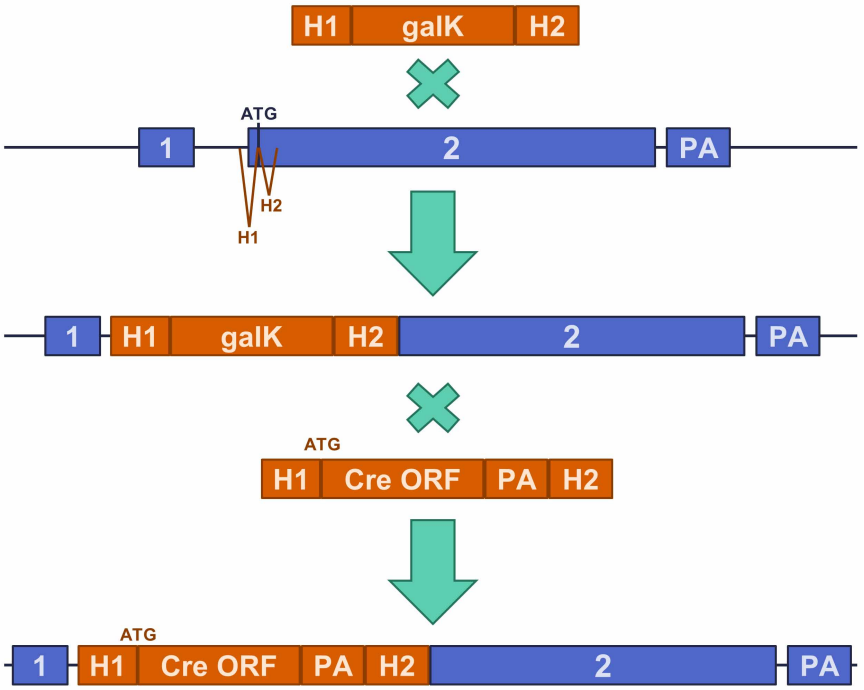

Extended Data Figure 1 | Generation of *Amigo2-Cre* mouse line. λ Red-mediated homologous recombination with galK positive and negative selection was used to make seamless changes to the bacterial artificial chromosome (BAC). PCR cassettes are shown in orange, and *Amigo2* locus is shown in blue. The PCR cassette contained two homology arms (H1, 58 nucleotides; H2, 62 nucleotides) that flanked the galactose kinase (galK) cassette. The homology arms flanked the *Amigo2* start codon. Recombination followed by positive selection was used to obtain the galK integrate. Recombination of the modified BAC with a PCR cassette containing the Cre open reading frame (ORF) and poly(A) (PA) flanked by the same homology arms yielded the final BAC used to generate the transgenic line.

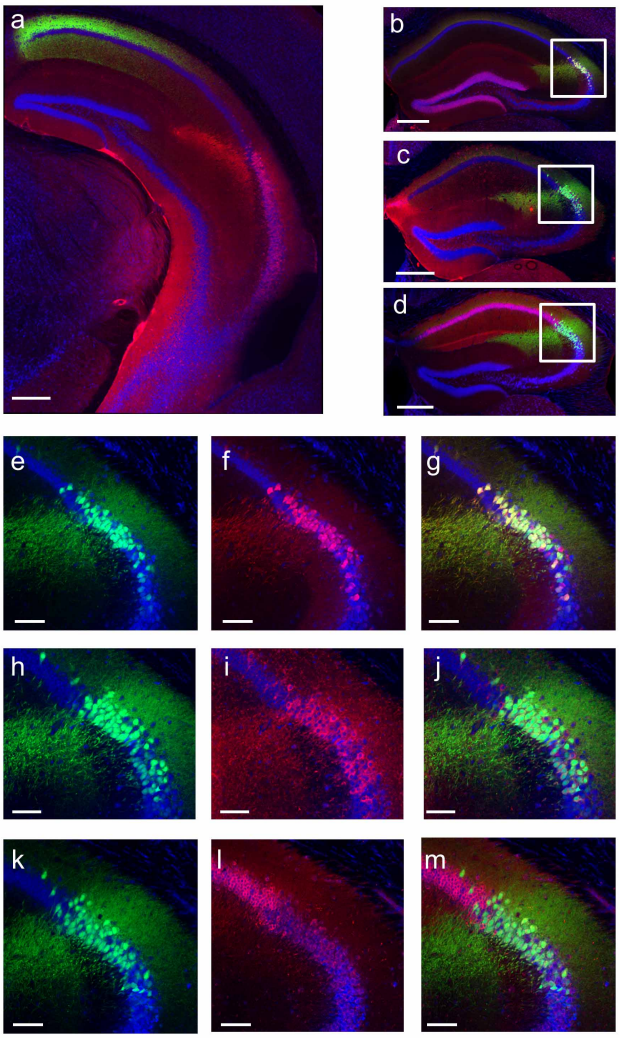

Extended Data Figure 2 | *Amigo2-Cre* mice express Cre in a genetically defined population of CA2 PNs. Coronal sections of hippocampus from *Amigo2-Cre* mice injected in dorsal hippocampus with a Cre-dependent AAV to express YFP (shown in green) in CA2. **a**, Coronal section of ventral hippocampus (about 2.8 mm caudal to bregma; see Fig. 54 of ref. 9 for a reference image) showing CA2 axons (green) from dorsal CA2. Note absence of YFP from ventral CA2 neurons (RGS14 stain in red). **b**, 97.22 ± 0.46% of YFP^+ cells ($n = 4$ mice, 2,948 cells) express the CA2 marker PCP4 (red). **c**, 98.45 ± 0.33% of YFP^+ cells ($n = 4$ mice, 2,870 cells) express the CA2 marker STEP (red). **d**, Almost no YFP^+ cells (0.17 ± 0.13%; $n = 4$ mice, 2,870 cells) express the CA1 marker WFS1 (red). **e**–**g**, Magnification of boxed area in **b**, showing YFP signal (**e**), PCP4 staining (**f**) and a merge of the two (**g**). **h**–**j**, Magnification of boxed area in **c**, showing YFP signal (**h**), STEP staining (**i**) and a merge of the two (**j**). **k**–**m**, Magnification of boxed area in **d**, showing YFP signal (**k**), WFS1 staining (**l**) and a merge of the two (**m**). Nissl stain shown in blue. Scale bars, 400 μm (**a**–**d**); 100 μm (**e**–**m**).

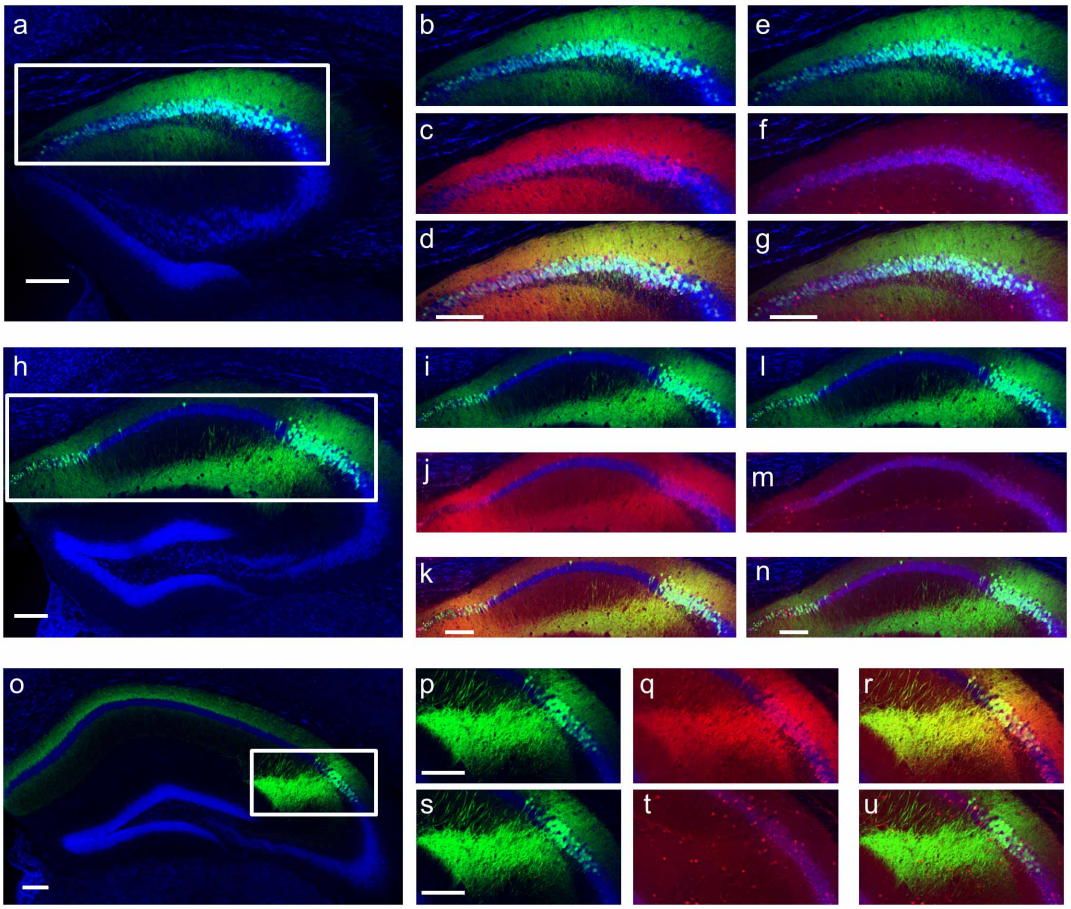

Extended Data Figure 3 | *Amigo2-Cre* mice express Cre in RGS14$^+$ CA2 PNs but not in GABA$^+$ inhibitory neurons. Cre$^+$ neurons expressing YFP (shown in green) co-label with RGS14 staining (shown in red), but do not co-label with GABA staining (shown in red in separate images). **a**, Reproduction of section −1.06 mm shown in Fig. 1b. **b**, **e**, Magnification of boxed area in **a**. **c**, RGS14 staining of section shown in **b**. **d**, Merge of **b** and **c**, showing YFP and RGS14 co-labelling. **f**, GABA staining of section shown in **e**. **g**, Merge of **e** and **f**, showing no overlap of GABA and YFP. **h**, Reproduction of section −1.46 mm shown in Fig. 1b. **i**, **l**, Magnification of boxed area in **h**. **j**, RGS14 staining of section shown in **i**. **k**, Merge of **i** and **j**, demonstrating YFP and RGS14 co-labelling. **m**, GABA staining of section shown in **l**. **n**, Merge of **l** and **m**, showing no overlap of GABA and YFP. **o**, Reproduction of section −2.18 mm shown in Fig. 1b. **p**, **s**, Magnification of boxed area in **o**. **q**, RGS14 staining of section shown in **p**. **r**, Merge of **p** and **q**, demonstrating YFP and RGS14 co-labelling. **t**, GABA staining of section shown in **s**. **u**, Merge of **s** and **t**, showing no overlap of GABA and YFP. Scale bars, 200 μm. Nissl stain shown in blue.

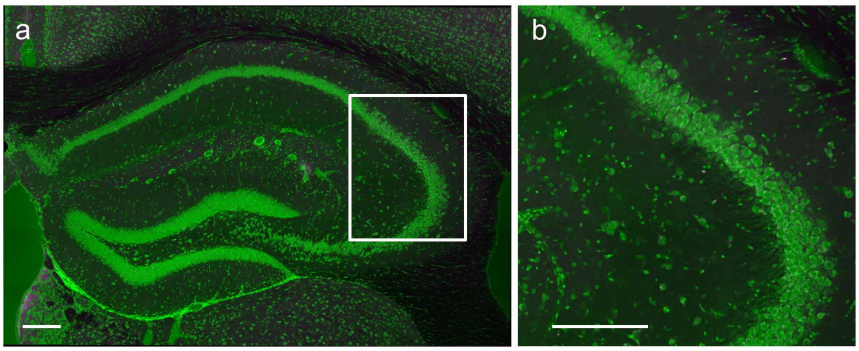

Extended Data Figure 4 | Specificity of the pseudotyped rabies virus. **a**, **b**, No labelled cells were observed ($n = 3$ mice) after injection of the (EnvA)SAD-ΔG-mCherry virus when TVA was not expressed in CA2. **b**, Magnification of boxed area in **a**. Rabies labelling would have appeared in magenta; Nissl stain shown in green. Scale bars, 200 μm.

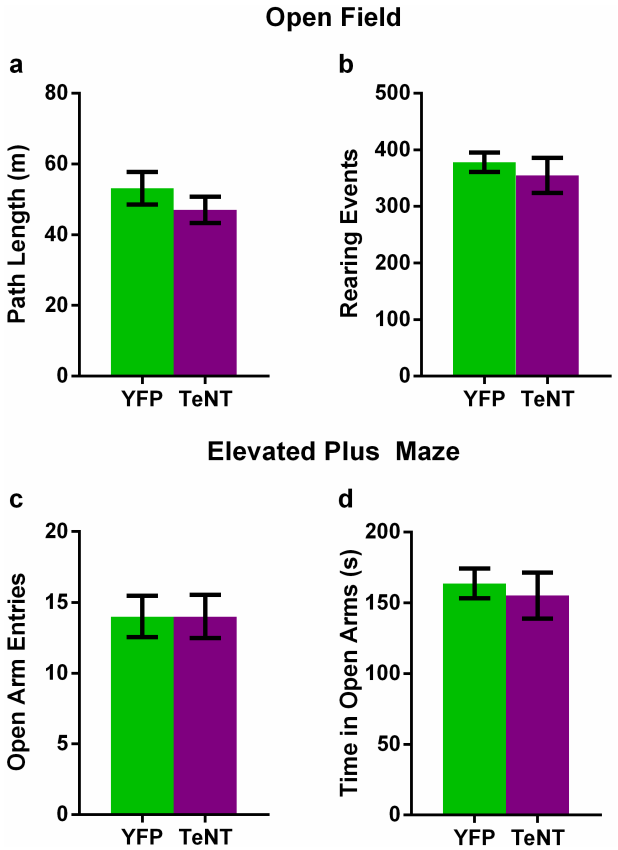

Extended Data Figure 5 | Inactivation of CA2 does not alter locomotor activity or anxiety-like behaviour. **a**, There was no significant difference ($P = 0.31$, two-tailed unpaired Student's *t*-test) between CA2-YFP and CA2-TeNT groups in the distance travelled in the open field (OF) test (YFP, 53.14 ± 4.62 m, $n = 8$; TeNT, 47.04 ± 3.70 m, $n = 10$). **b**, There was also no significant difference ($P = 0.55$, two-tailed unpaired Student's *t*-test) between the groups in the number of rearing events recorded during the OF session (YFP, 378.0 ± 17.36, $n = 8$; TeNT, 354.7 ± 30.99, $n = 10$). **c**, **d**, Inactivation of CA2 did not alter anxiety-like behaviour measured in the elevated plus maze (EPM). The number of open arm entries was not significantly different ($P > 0.99$, two-tailed unpaired Student's *t*-test) between the groups (YFP, 14.00 ± 1.46, $n = 8$; TeNT, 14.00 ± 1.54, $n = 10$). Additionally, the time spent in the open arms (YFP, 163.7 ± 10.43 s, $n = 8$; TeNT, 155.1 ± 16.38 s, $n = 10$) did not differ significantly ($P = 0.68$, two-tailed unpaired Student's *t*-test) between the groups. Results are means ± s.e.m.

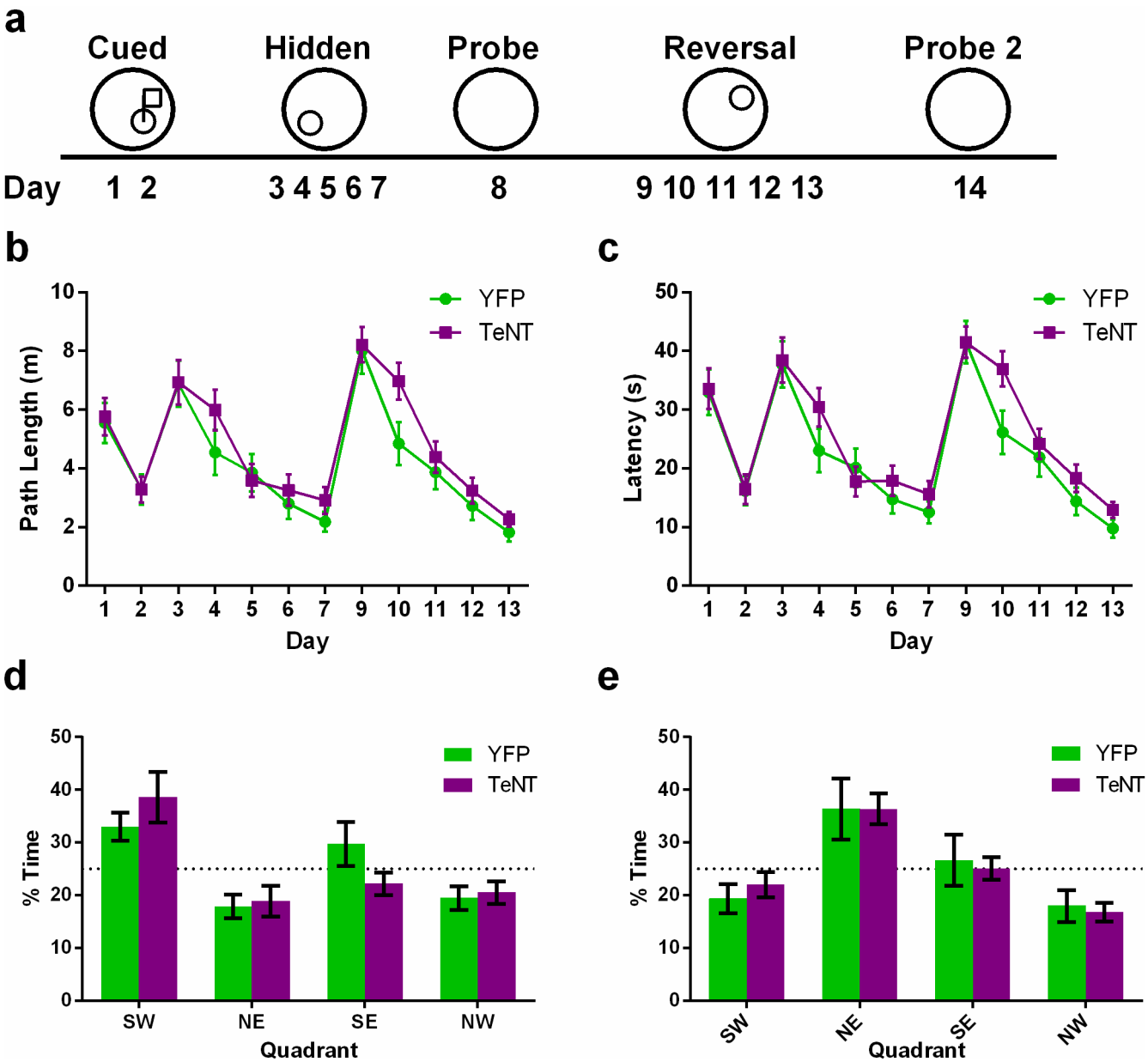

Extended Data Figure 6 | Spatial learning and memory assayed with the Morris water maze task is unaltered by CA2 inactivation. **a**, Diagram of the experimental design. On days 1 and 2 mice were trained to find a platform with a visible flag. On days 3–7 mice were trained to find a hidden platform located in the southwest quadrant of the water maze. Spatial memory was assayed on day 8 with the platform removed. Reversal training was conducted on days 9–13 with the platform now hidden in the northwest quadrant. Spatial memory of the novel location was tested on day 14. **b**, Path length to the platform was not altered significantly by CA2 inactivation (two-way repeated-measures ANOVA: treatment × time $F(11,770) = 0.67$, $P = 0.77$; time $F(11,770) = 21.87$, $P < 0.0001$; treatment $F(1,70) = 2.85$, $P = 0.10$). **c**, Latency to find the platform did not differ significantly between the two groups (two-way repeated-measures ANOVA: treatment × time $F(11,770) = 0.78$, $P = 0.66$; time $F(11,770) = 25.23$, $P < 0.0001$; treatment $F(1,70) = 2.84$, $P = 0.10$). YFP, $n = 8$; TeNT, $n = 10$. **d**, Spatial memory during the probe trial was unaffected by CA2 inactivation. The percentage of time spent in the target quadrant (YFP, 33.00 ± 2.66%; TeNT, 38.6 ± 4.79%) was not significantly different between the two groups ($P = 0.36$, two-tailed unpaired Student's *t*-test). **e**, Spatial memory after reversal training was unaffected by CA2 inactivation. There was no significant difference between the groups in the percentage of time spent in the target quadrant during the probe trial after reversal training (YFP, 36.38 ± 5.75%; TeNT, 36.40 ± 2.92%; $P > 0.99$, two-tailed unpaired Student's *t*-test). Results are means ± s.e.m.

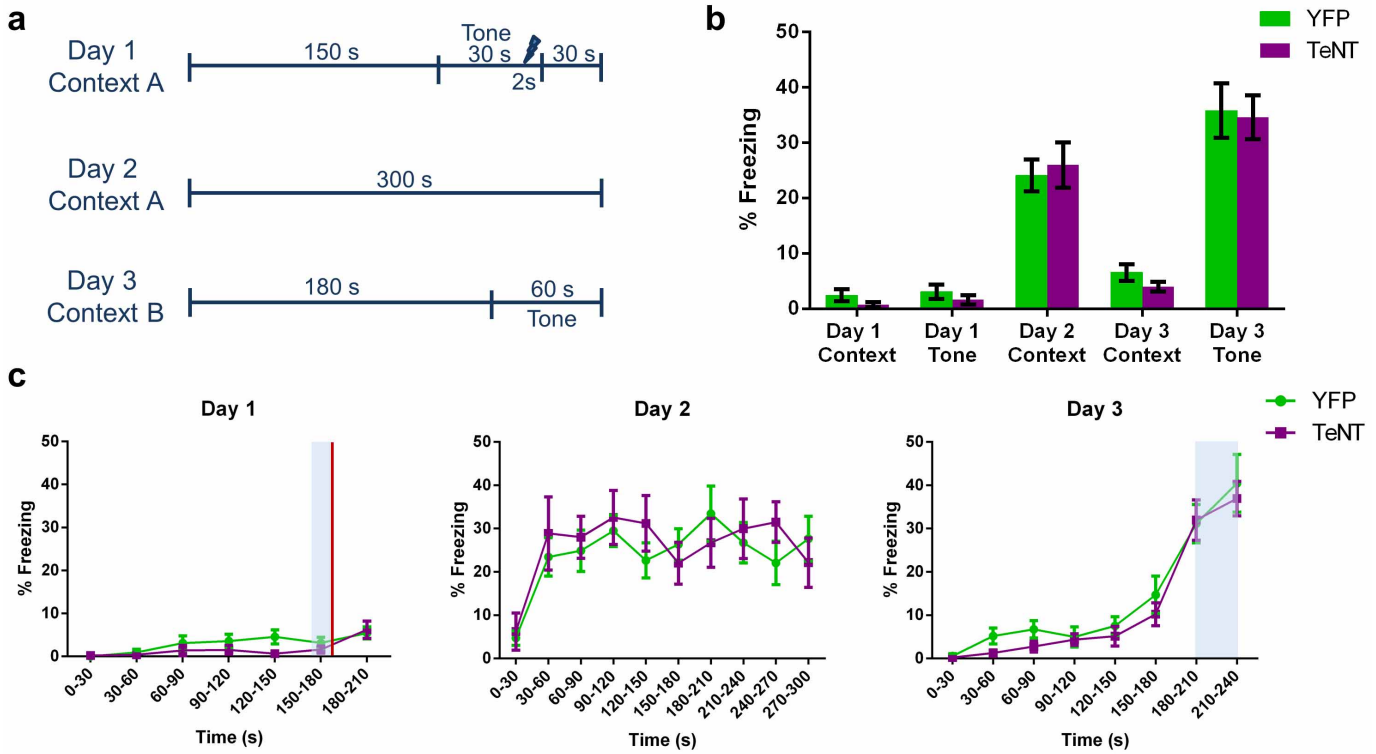

Extended Data Figure 7 | Contextual fear-conditioning memory and auditory fear-conditioning memory are unaffected by inactivation of CA2. **a**, Diagram of the experimental design. Delay fear conditioning was employed to test hippocampus-dependent contextual fear memory and amygdala-dependent auditory fear memory. **b**, There was no significant difference in percentage freezing between the groups (two-way repeated-measures ANOVA: treatment × day $F(4,68) = 0.31$, $P = 0.87$; treatment $F(1,17) = 0.13$, $P = 0.73$; day $F(4,68) = 100.8$, $P < 0.0001$; YFP, $n = 11$; TeNT, $n = 8$). Before training on day 1, neither group showed a fear response to context A (YFP, 2.45 ± 1.06%; TeNT, 0.75 ± 0.49%) or to the tone (YFP, 3.09 ± 1.31%; TeNT, 1.63 ± 0.84%). On day 2 after training, robust fear responses to context A were measured in both groups (YFP, 24.09 ± 2.88%; TeNT, 26.00 ± 4.10%). Both groups showed low levels of freezing on day 3 in novel context B (YFP, 6.55 ± 1.52%; TeNT, 4.00 ± 0.87%), demonstrating context specificity of the fear memory and a lack of fear generalization. Both groups showed robust freezing to the tone on day 3 (YFP, 35.82 ± 4.93%; TeNT, 34.63 ± 3.96%), demonstrating intact auditory fear memory. **c**, Freezing data plotted in 30-s bins. Shaded areas represent tone presentation. Red line represents shock delivery. Left: two-way repeated-measures ANOVA revealed no significant difference between groups in freezing on day 1 (treatment × time $F(6,102) = 1.135$, $P = 0.3474$; treatment $F(1,17) = 1.116$, $P = 0.3056$; time $F(6,102) = 6.348$, $P < 0.0001$). Middle: two-way repeated-measures ANOVA revealed no significant difference between groups in freezing on day 2 (treatment × time $F(9,153) = 0.9741$, $P = 0.4637$; treatment $F(1,17) = 0.1326$, $P = 0.7203$; time $F(9,153) = 6.335$, $P < 0.0001$). Right: two-way repeated-measures ANOVA revealed no significant difference between groups in freezing on day 3 (treatment × time $F(7,119) = 0.2490$, $P = 0.9716$; treatment $F(1,17) = 0.6517$, $P = 0.4307$; time $F(7,119) = 50.87$, $P < 0.0001$). Results are means ± s.e.m.

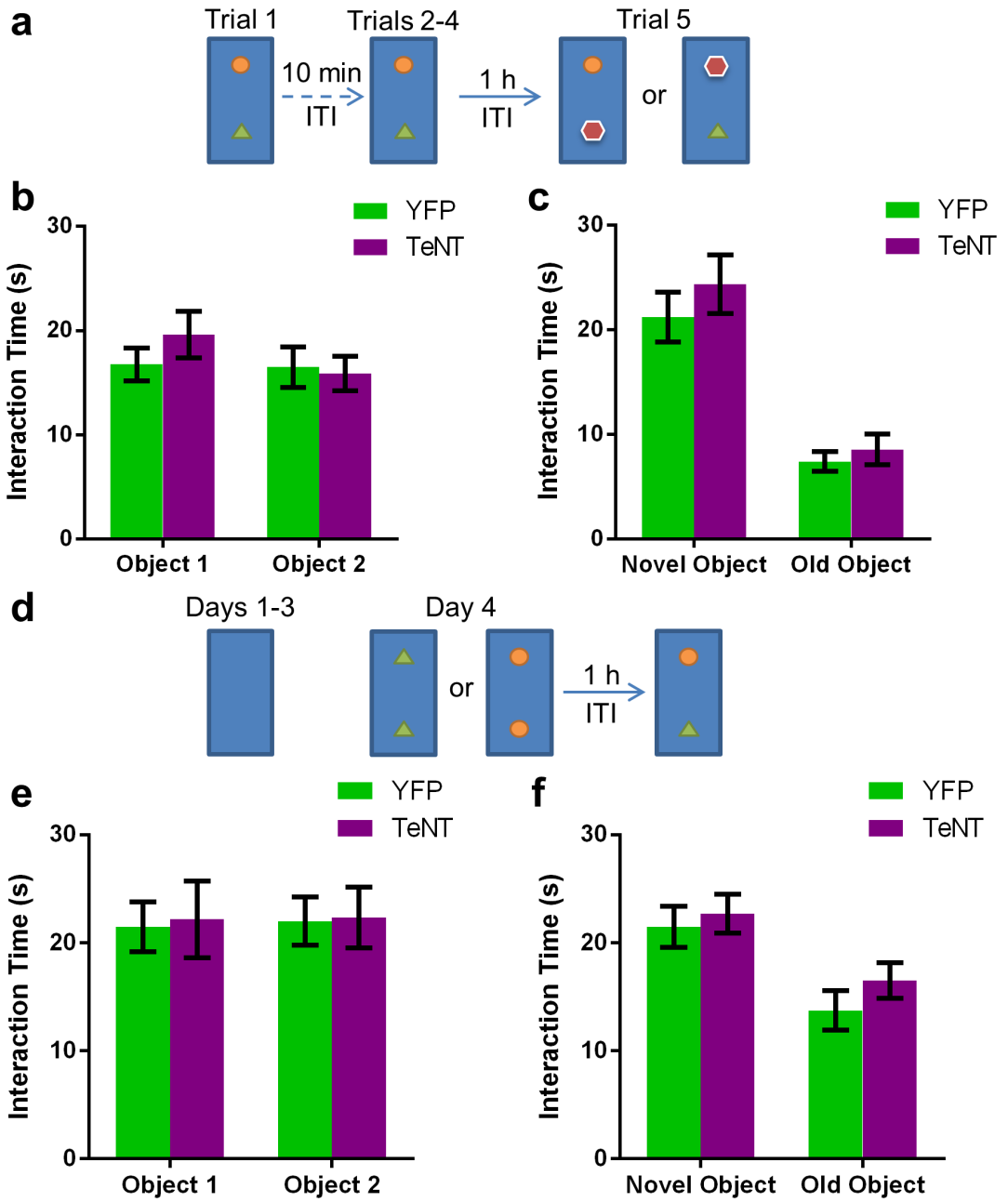

Extended Data Figure 8 | Object recognition memory and preference for novelty is preserved in CA2-TeNT animals. **a**, Diagram of the experimental design for the novel-object-recognition task. **b**, The groups did not differ significantly in exploration of object 1 (YFP, 16.75 ± 1.57 s; TeNT, 19.60 ± 2.24 s) or object 2 (YFP, 16.50 ± 1.97 s; TeNT, 15.90 ± 1.66 s) averaged over the course of the first four trials (two-way ANOVA: treatment × object $F(1,32) = 0.80$, $P = 0.38$; object $F(1,32) = 1.05$, $P = 0.31$; treatment $F(1,32) = 0.34$, $P = 0.56$; YFP, $n = 8$; TeNT, $n = 10$). **c**, Both groups explored the novel object (YFP, 21.23 ± 2.37 s; TeNT, 24.37 ± 2.81 s) more than the familiar object (YFP, 7.41 ± 0.92 s; TeNT, 8.57 ± 1.48 s). Statistical analysis revealed a significant effect of object, but not CA2 inactivation or interaction of the two (two-way ANOVA: treatment × object $F(1,28) = 0.22$, $P = 0.64$; object $F(1,28) = 48.46$, $P < 0.0001$; treatment $F(1,28) = 1.02$, $P = 0.32$). Multiple comparison testing revealed a significant difference between exploration of the novel object compared with exploration of the old object for both the YFP group ($P = 0.0002$) and the TeNT group ($P < 0.0001$). **d**, Diagram of the experimental design for another variation of the novel-object-recognition task. **e**, The groups did not differ significantly in time spent exploring object 1 (YFP, 21.50 ± 2.31 s; TeNT, 22.18 ± 3.57 s) or object 2 (YFP, 22.02 ± 2.23 s; TeNT, 22.36 ± 2.81 s) during trial 1 of day 4 (two-way ANOVA: treatment × object $F(1,44) = 0.004$, $P = 0.95$; object $F(1,44) = 0.02$, $P = 0.90$; treatment $F(1,44) = 0.03$, $P = 0.85$; YFP, $n = 12$; TeNT, $n = 12$). **f**, Both groups explored the novel object (YFP, 21.49 ± 1.91 s; TeNT, 22.73 ± 1.82 s) more than the familiar object (YFP, 13.74 ± 1.83 s; TeNT, 16.53 ± 1.64 s). Statistical analysis revealed a significant effect of object, but not CA2 inactivation or interaction of the two (two-way ANOVA: treatment × object $F(1,44) = 0.18$, $P = 0.67$; object $F(1,44) = 15.02$, $P = 0.0004$; treatment $F(1,44) = 1.25$, $P = 0.27$). Multiple comparison testing revealed a significant difference between exploration of the novel object compared with exploration of the old object for both the YFP group ($P = 0.008$) and the TeNT group ($P = 0.02$). Results are means ± s.e.m.

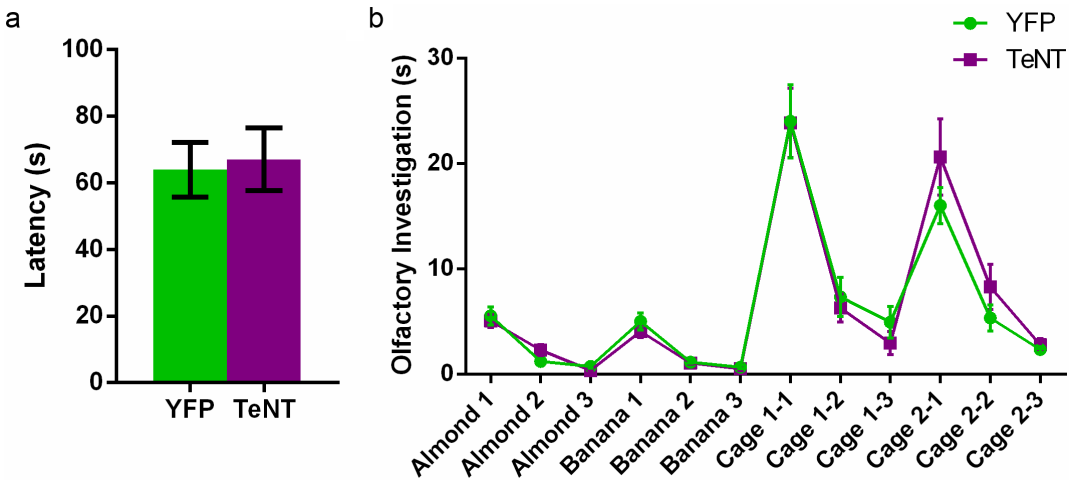

Extended Data Figure 9 | Olfaction is unaffected by CA2 inactivation. **a**, There was no significant difference between the groups in latency to find a buried food pellet (YFP, 63.93 ± 8.22 s, $n = 15$; TeNT, 67.06 ± 9.42 s, $n = 16$; $P = 0.81$, two-tailed unpaired Student's t-test). **b**, There was no significant difference between the groups (YFP, $n = 15$; TeNT, $n = 14$) in performance on the olfactory habituation/dishabituation task (two-way repeated-measures ANOVA: treatment × trial $F(11,297) = 0.933$, $P = 0.51$; treatment $F(1,27) = 0.08$, $P = 0.78$; trial $F(11,297) = 60.21$, $P < 0.0001$). Results are means ± s.e.m.

Extended Data Table 1 | Electrophysiological properties of Cre$^+$ neurons

Extended Data Table 1 | Electrophysiological properties of Cre$^+$ neurons

	Cre$^+$ neurons	CA1	P value
Input Resistance (MΩ)	68.3 ± 3.03	90.0 ± 6.65	0.039
Capacitance (pF)	296.0 ± 18.68	140.7 ± 8.02	< 0.0001
Resting Potential (mV)	-76.3 ± 0.63	-72.8 ± 0.92	0.024
AP Amplitude (mV)	90.81 ± 2.17	99.15 ± 1.36	0.007
AP Duration (ms)	0.83 ± 0.02	1.06 ± 0.06	0.031
Sag (mV)	1.92 ± 0.50	7.55 ± 0.85	0.0006

The electrophysiological properties of Cre$^+$ neurons (column 1) closely matched the properties previously reported[7] for CA2 neurons, and differed significantly from the properties of CA1 neurons (column 2). Two-tailed unpaired Student's *t*-tests were used to assess significant differences between the neuronal populations. The *P* values are shown in column 3. Whole-cell recordings of Cre$^+$ ($n = 5$) and CA1 ($n = 9$) neurons were conducted to measure input resistance, capacitance, resting potential, action potential (AP) amplitude, AP duration, and sag. Input resistance and capacitance were measured with a −5-mV pulse. The amplitude and duration of the AP were measured during a 500-ms depolarizing pulse, and the sag resulting from the activation of I_h was measured during a 500-ms hyperpolarization from −70 mV to −100 mV. The smaller sag in Cre$^+$ neurons than that previously reported[7] was probably due to differences in the extent of whole-cell dialysis resulting from differences in recording protocols.